# First direct measurement of sticking in d tCF

M. A. Paciotti, O. K. Baker, J. N. Bradbury, J. S. Cohen, M. Leon, H. R. Maltrud, L. L. Sturgess, S. E. Jones, P. Li, L. M. Rees, E. V. Sheely, J. K. Shurtleff, S. F. Taylor, A. N. Anderson, A. J. Caffrey, J. M. Zabriskie, F. D. Brooks, W. A. Cilliers, J. D. Davies, J. B. A. England, G. J. Pyle, G. T. A. Squier, A. Bertin, M. Bruschi, M. Piccinini, A. Vitale, A. Zoccoli, V. R. Bom, C. W. E. van Eijk, H. de Haan, and G. H. Eaton

Citation: AIP Conference Proceedings **181**, 38 (1988); doi: 10.1063/1.37880
View online: http://dx.doi.org/10.1063/1.37880
View Table of Contents:
http://scitation.aip.org/content/aip/proceeding/aipcp/181?ver=pdfcov
Published by the AIP Publishing

# FIRST DIRECT MEASUREMENT of $\alpha - \mu$ STICKING in $dt - \mu$CF

M.A. Paciotti, O.K. Baker, J.N. Bradbury, J.S. Cohen, M. Leon,
H.R. Maltrud, L.L. Sturgess,
Los Alamos National Laboratory, Los Alamos, N.M.,

S.E. Jones, P. Li, L.M. Rees, E.V. Sheely, J.K. Shurtleff, S. F. Taylor,
Brigham Young University, Provo, Utah,

A.N. Anderson,
Idaho Research, Boise, Idaho,

A.J. Caffrey, J.M. Zabriskie
Idaho National Engineering Laboratory, Idaho Falls, Idaho

F.D. Brooks, W.A. Cilliers, J.D. Davies, J.B.A. England, G.J. Pyle, G.T.A. Squier,
University of Birmingham, Chilton, England

A. Bertin, M. Bruschi, M. Piccinini, A. Vitale, A. Zoccoli,
University of Bologna, Bologna, Italy

V.R. Bom, C.W.E. van Eijk, H. de Haan,
Delft University of Technology, Holland, and

G.H. Eaton,
Rutherford-Appleton Laboratory,
Didcot, Oxfordshire.

## ABSTRACT

Both $(\alpha\mu)^+$ and $\alpha$ particles have been observed in coincidence with fusion neutrons in a gaseous $D - T$ target at $2.8 \times 10^{-3}$ liquid-hydrogen density. The initial muon sticking probability in muon-catalyzed $d - t$ fusion, measured directly for the first time, is $(0.80 \pm 0.15 \pm 0.12$ systematic)% in agreement with 'standard' theoretical calculations. However, this measured value does not support those theories that invoke special mechanisms to alter the initial sticking value.

## INTRODUCTION

There has been a need for some time for a direct measurement of the $\alpha - \mu$ sticking probability in muon-catalyzed $d - t$ fusion.[1] The muon loss due to this sticking phenomenon is the most severe limitation to the ultimate fusion yield $\chi$. The sticking probability, $\omega_s$, has been inferred from the total muon loss rate after detailed corrections[2,3,4,5], and from x-ray measurements[6,7] plus cascade calculations[8,9]. Vorobyov expects that the LNPI direct ionization chamber method, so successful in $dd - \mu CF$, will work for measuring sticking in $dt - \mu CF$;[10] so far an upper limit of 1% comes from this work.[11]

The present paper describes the first direct measurement of the $\alpha - \mu$ sticking probability, using a low density ($\approx 10^{-3}$ $lhd$) $D - T$ mixture.[12] As such, it comes very close to measuring the initial sticking probability in $dt - \mu CF$. Extension of the this work is presently underway at Rutherford-Appleton Laboratory (RAL).[13]

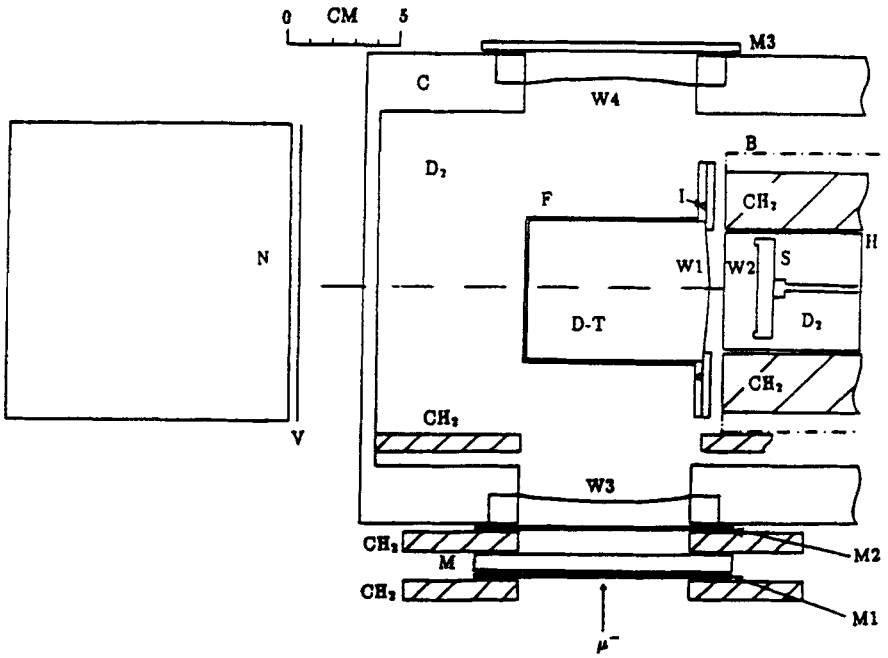


Fig. 1.

F: Beryllium target flask, 6.4 cm diameter, 7.6 cm long; cylindrical walls are 1.5 mm thick; contains $D - T$,$C_t = 0.4$.
W1,W2: 1.5 micron mylar windows aluminized 1600 $\mathring{A}$ on $T_2$ side.
I: Pure indium 'O'-ring sealing the target window.
S: Silicon surface barrier detector, 1000 mm$^2$, 100 microns thick.
M1,M2,M3: Muon telescope counters, each 1.6 mm thick
N: Neutron counter, Bicron liquid scintillator (BC-501), 12.7 $cm$ in diameter and 12.7 cm in depth; 1.6 mm veto counter in front.
B: Dotted line indicates poletip of 1 kG permanent magnetic field.
C: Secondary container for $D_2$, 12 $l$ volume, Al walls, Lucite lid, all seals Viton 'O'-rings.
W3,W4: Heat treated Al beam entrance and exit windows, 0.13 mm thick.
H: Detector housing, sealed, cooled, and moveable; contains $D_2$.
M: Moderator for slowing down 60-MeV/c $\mu^-$ beam.
V: Charged particle veto counter.

## The CONCEPT of the LAMPF EXPERIMENT

The $(\alpha\mu)^+$ ions produced by "sticking" events and the $\alpha$-particles formed in the remaining $99^+$ % majority of events are detected in coincidence with the 14.1 MeV neutron and are easily separable by range in the low pressure $D-T$ gas; the density is dictated by the very limited ranges of these ions. The fact that the ions are produced at 180° from the neutrons is useful for background rejection. Triggers due to $(\mu^-, pn)$ and $(\mu^-, p2n)$ captures in the target flask are substantially suppressed since the charged particle is not similarly correlated in angle with the neutron[14]. Beryllium, chosen for its good properties in containing tritium and its very low muon-capture probability, is the best target material for use in the LAMPF beam structure. The full $\mu^-$ beam is directed on the target to achieve an adequate event rate; many muons are therefore present in the target at one time, and there is then almost no possibility to measure the fusion time with respect to the muon arrival time. (This will be possible using the RAL pulsed muon beam.) Even though high-Z materials do not exhibit many charged particles in coincidence with neutrons, the high capture probability produces overwhelming singles rates in both neutron and silicon detectors.

## LAYOUT

Features of the setup are shown in Fig. 1. Most important, the silicon detector must be protected from tritium beta radiation. $T_2$ diffuses out through the target window W1, limited primarily by the aluminum coating, at a measured rate of 2.5% per day and is diluted by the large volume of the secondary container. The second window W2 then keeps this dilute mixture at a distance from the detector where the intervening $D_2$ region is guarded by a magnetic field. The detector housing is sealed except for a long pressure-equilibrating capillary, necessary when the detector housing is cooled; cooling to $-7°$ C improved the timing resolution from 3.5 to 3.0 ns. Target filling is challenging since the windows cannot support much differential pressure; as a molecular sieve cold trap cleans the incoming premixed $D-T$ gas, $D_2$ is admitted to the secondary container at a rate that maintains low differential pressure. Backgrounds are measured in an identical apparatus filled entirely with $D_2$ and normalized to incoming muons. A $^{233}U$ source, insertable between W1 and W2, gave identical energy and timing calibrations for each apparatus.

The character of the LAMPF experiment is revealed by typical rates; both peak rates during the LAMPF pulse and average rates are given in Table I. (During this particular run period, a thin production target caused the rates to be reduced by a factor of 3 below normal.) The neutron rate $n$ is taken after pulse-shape discrimination[15]; the $\alpha$ rate includes noise; $\alpha \cdot (\gamma + n)$ is the trigger rate formed with a 150 ns coincidence width. Clearly the fusion process in not observable in either the neutron or the $\alpha$-singles rate.

TABLE I. Typical rates.

| *RATE* | *M1M2M3* | $\gamma + n$ | $n$ | $\alpha$ | $\alpha \cdot (\gamma + n)$ |
|---|---|---|---|---|---|
| *Peak/s* | $2.6 \times 10^6$ | $1.5 \times 10^4$ | 560 | 1440 | 2.8 |
| *Average/s* | $1.4 \times 10^4$ | 810 | 30 | 80 | 0.15 |

## SYSTEMATIC EFFECTS

The factor 4 ratio between $(\alpha\mu)^+$ and $\alpha$ ranges was utilized by two different schemes; in an earlier experiment both ions were detected concurrently, while for the latest data, optimum detection of each ion required different fill pressures. Table II compares merits and systematic effects for each method. At 650 Torr the experiment is severely rate-limited and (at LAMPF) background-limited. We could not have been certain that $(\alpha\mu)^+$ had been seen without a higher density run. Using the dual pressure scheme, a strong $(\alpha\mu)^+$ signal is seen. However, the usefulness of the data may be limited by the systematic uncertainty of yield $\chi$ scaling with density $\phi$. This scheme presents a good opportunity to measure stripping effects.

TABLE II. Systematic effects.

*$(\alpha\mu)^+$ and $\alpha$ detected concurrently :*

1) Single fill, $\phi = 1.0 \times 10^{-3}$ *lhd*, 650 Torr.
2) $\alpha$'s are collected from only 1/2 of target volume nearest the window.
3) $\mu^-$ stopping distribution must be well known.
4) $\alpha$ ranges must be known very well.
5) Gas impurity only affects the fusion yield $\chi$ , not the sticking result.
6) Slightly lower stripping since $(\alpha\mu)^+$ energies are higher.
7) No $t\mu$, $d\mu$ diffusion effect.
8) $C_t$ only alters the yield $\chi$.

*Separate $D-T$ fills for $(\alpha\mu)^+$ and $\alpha$ observation :*

1) Two fills, $\phi = 7.6 \times 10^{-4}$ $(490\ Torr)\alpha$ and $\phi = 2.8 \times 10^{-3}(1800\ Torr)(\alpha\mu)^+$.
2) Both ions are collected from the full target volume.
3) Assume muon stopping rate and distribution scales with density $\phi$. The $\mu^-$ stopping distribution only comes into stripping and diffusion corrections.
4) Most uncertainty in range cancels out.
5) Gas impurity necessitates an important systematic correction.
6) Stripping is higher but still well known.
7) $t\mu$ and $d\mu$ may diffuse to the walls at the low density.
8) $C_t$ change due to tritium diffusing out the window will alter the fusion yield at each pressure and thereby confuse the normalization.

A Monte Carlo code is useful for evaluating these systematic effects, but the experiment is not so complicated that the code is essential to the analysis. Figure 2 displays the distributions of fusion events in the dual-pressure scheme, reflecting principally the muon stopping distribution, detector solid angles, and particle range. $\alpha$-particles originating near the back of the flask fall below the 0.7 MeV threshold and are not detected. The code finds a 93% active volume, whereas the $(\alpha\mu)^+$ active volume is 100%. According to the prescription, we could have used about 460 Torr to avoid this correction, but we favored instead a slightly higher density to obtain a higher $\chi$. The overall efficiency is small (0.08% per stopped $\mu^-$), independent of density, and, aside from the volume correction, cancels out of the sticking result.

Variation in the muon stopping intensity within the target volume was measured by counting the $^{56}$Mn activation[16] of thin iron foils placed inside the non-tritiated target. Compared with the central maximum, the intensity falls to 1/2 along the axis near the window and the back wall. The predicted stop rate in hydrogen, based on these foils, was $4.7 \times 10^{-4}$ $\mu^-$ stopped per incident $\mu^-$ at 490 Torr.

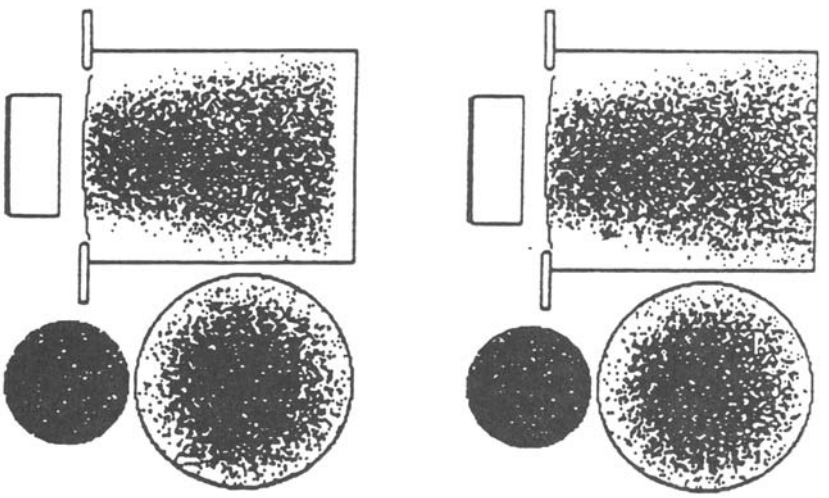

Fig. 2. Left side: 490 Torr; $\alpha$. Active volume is 93% of target volume. Right side: 1800 Torr; $(\alpha\mu)^+$ ions are detectable from the full target volume. Here, the $\alpha$'s , having about 1/4 the range of the $(\alpha\mu)^+$ ions, are below threshold. The $\alpha$ locus at the detector and the projection along the target axis of the fusion distribution are shown below.

The Monte Carlo uses the Bichsel range code,[17] which was verified by degrading five $\alpha$ energies from the $^{233}U$ source through various gas thickness obtained by moving the detector. These checks were done between data runs uti-

lizing the same windows and fill gas as fusion particles. Good consistency was obtained, and we conclude that the calculated range of a 3.5-MeV $\alpha$ degraded to the 0.7 MeV threshold was verified to about 2 mm.

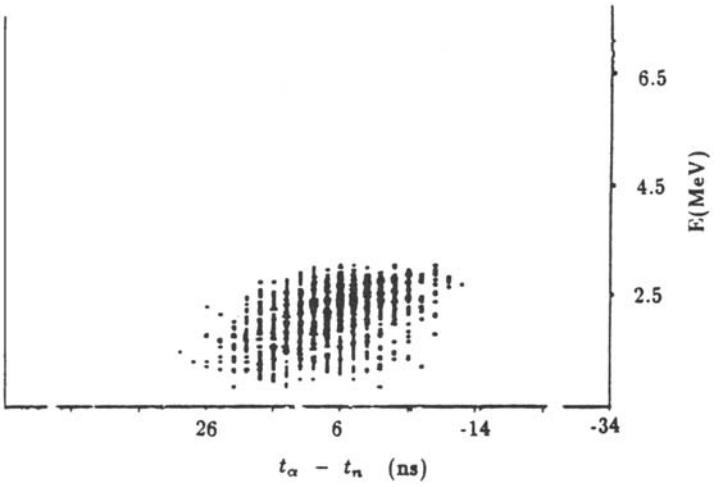


Fig. 3. Monte Carlo prediction for $(\alpha\mu)^+$ at 1800 Torr. Time vs energy correlation is evident. The higher energy $(\alpha\mu)^+$'s arrive early.

Corrections for stripping are easily and accurately given by the Monte Carlo using the energy-dependent stripping cross sections for $D-T$ gas, aluminum, mylar, and $D_2$ gas.[18] Table III lists stripping for the several materials assuming an average energy at each position. It can be used to assess the relative effect of the gas and of the windows, which are approximately equal.

TABLE III. Stripping probabilities.

| *STRIPPING MATERIAL* | *STRIPPING PROBABILITY* |
|---|---|
| 3.9 *cm avg.* $D-T$ *pathlength at* 1800 *Torr* | 6.5% |
| 1600 Å Al coating on target window | 1.3% |
| 1.5 *micron mylar target window* | 4.0% |
| 1.0 *cm* $D_2$ *at* 1800 *Torr* | 1.0% |
| 1600 Å Al coating on detector window | 1.1% |
| 1.5 *micron mylar detector window* | 3.9% |
| 1.5 *cm* $D_2$ *at* 1800 *Torr* | 2.1% |

However note that many of the stripped $(\alpha\mu)^+$ still have enough energy to be detected above threshold as $\alpha$ particles, particularly if the stripping occurs in

the detector window or the last 1.5-cm $D_2$ region. The net result after the code has considered all of the above (stopping distribution, solid angle, energy loss, stripping at proper energies, and detection threshold) is that only 16% of the initially produced $(\alpha\mu)^+$ are unobserved. This effective stripping, $R_{eff} = 0.16$, is quite small considering that more efficient strippers such as aluminum and mylar have been introduced. Stripping is significantly less than that seen when the ion is allowed to stop fully in a medium[8], and convinces us that initial sticking is close at hand in this direct method. Verification of stripping calculations could be accomplished in these experiments, for example, by testing the effect of additional mylar. Reduced backgrounds at RAL will also be helpful. Fusion $\alpha$ particles generated between W1 and W2 could simulate $(\alpha\mu)^+$ events; however, $C_t$ is so low there that the correction to $\omega_s^o$ is estimated to be much less than 1% of $\omega_s^o$ and is therefore neglected.

## DATA

The pulse-shape discrimination[15] picture is given in Fig. 4 showing the location of the cut that selects the approximately 4% neutron signal from the remaining $\gamma$'s that arise mainly from muon-decay electrons.

The $\alpha$-data are presented first since the signal is so prominent (Fig. 5). Only the neutrons have been selected, and prompt muons have been rejected. The time difference between the $\alpha$-ion and the fusion neutron is plotted along the abscissa while the ion energy is plotted along the ordinate. The box drawn shows the region where the $\alpha$'s are expected from Monte Carlo predictions. The position of the box along the time axis cannot be known from measurement, so the $\alpha$-data themselves are used as a guide to positioning the box. $(\alpha\mu)^+$ ions are also expected in this plot, but with such low rate that background masks them.

The $(\alpha\mu)^+$ spectrum for all data taken at 1800 Torr is shown in Fig. 6, where the axes are the same as in Fig. 5. A quick comparison with its companion background plot shows a strong signal, but of course not as clean as the $\alpha$ data. The coincident background, which extends from threshold to well above the maximum $(\alpha\mu)^+$ energy, comes from from $\mu^-$ capture in the beryllium target flask; protons, deuterons, tritons, and alphas, are emitted in coincidence with neutrons. Non-coincident background, in the wings of the time distribution, originates from a variety of sources producing singles, including scattered muons which cannot be completely rejected and products from $\mu^-$ capture in beryllium, polyethylene, and aluminum.

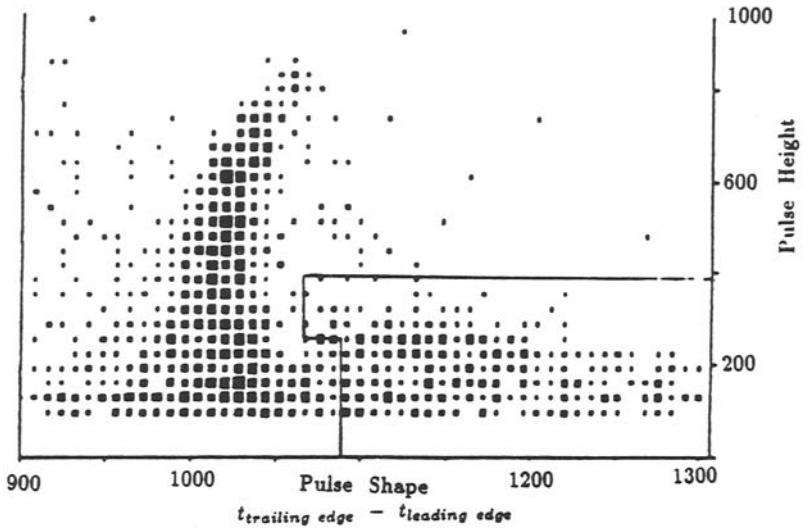


Fig. 4. Neutron separation by pulse shape.

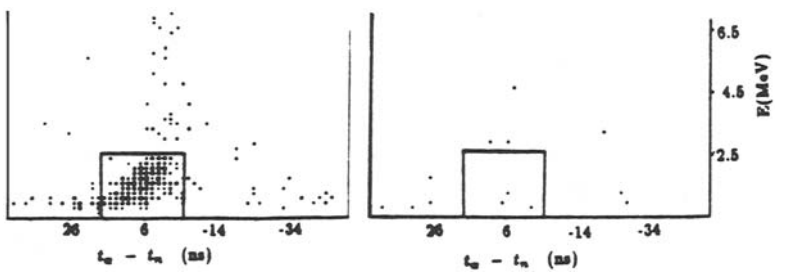


Fig. 5. $\alpha$ data on the left. Background on the right for 1/7 number of incident muons.

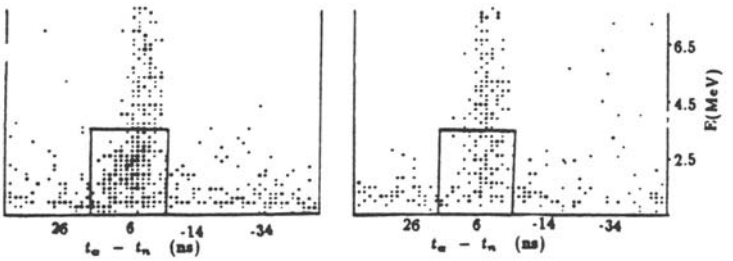


Fig. 6. The $(\alpha\mu)^+$ spectrum for all data taken at 1800 Torr. Background is shown on the right for 3/4 number of incident muons.

Table IV lists the raw numbers obtained from the data.

TABLE IV. Raw Data.

| *PRESSURE* | *REGION* | *COUNTS* | *M1.M2.M3* |
|---|---|---|---|
| 1800 *Torr* | $(\alpha\mu)^+$ | 115 | $16.7 \times 10^9$ |
| 1800 *Torr* | *Background* | 90 | $29.1 \times 10^9$ |
| 490 *Torr* | $\alpha$ | 295 | $7.2 \times 10^9$ |
| 490 *Torr* | *Background* | 3 | $1.05 \times 10^9$ |

## PURITY OF $D-T$ GAS

An anticipated source of trouble was impurities in the $D-T$ mixture. (See table II.) The mylar window precludes a high-temperature bakeout of the target, and there just is not enough gas to overpower small fixed amounts of contaminants as there is for the high-pressure targets.[12] The procedure used was to fill first to 1800 Torr and to collect $(\alpha\mu)^+$ data, then to bleed the gas pressure down to 490 Torr and collect $\alpha$ data. In this way, the same gas was used for the measurement and for the normalization. Time-dependent evolution of contaminants from the walls by tritium is not prevented by this procedure, but none was evident. A second 1800-Torr data run produced 30% more $(\alpha\mu)^+$ than did the first 1800-Torr fill when normalized to entering muons while no changes were evident in the background. It was not possible to accomplish the bleed procedure for this fill, and so confident normalization is lacking for more than 1/2 of the $(\alpha\mu)^+$ counts in Fig. 6. The direction of the observed effect is consistent with a cleaner mixture being obtained for the second fill following tritium scouring of the surfaces occuring during the first fill. Contamination

of the $D_2$ in the secondary container could also contaminate the target gas by diffusion through the window; we expect less such impurity for a second fill. Although the increase is not statistically conclusive, its direction reinforces our belief that it is due to a change in gas properties. Consequently, only the first set of runs at 1800 Torr were used in deriving the sticking probability, the data appearing in Table IV. If impurity did cause the change in $\chi$, we estimate about 600 ppm (with the Z of nitrogen) was present.

## RESULTS

The initial sticking probability is given by

$$\omega_s^o = \frac{N_{\alpha\mu}}{N_\alpha + N_{\alpha\mu}}. \qquad (1)$$

Here

$$N_{\alpha\mu} = \frac{n_{\alpha\mu}}{N\phi^2(1 - R_{eff})}, \qquad (2a)$$

$$N_\alpha = \frac{n_\alpha}{N\phi^2\ 0.93} \qquad (2b)$$

where $n_\alpha$ ($n_{\alpha\mu}$) is the number of doubly (singly) charged ions detected, $R_{eff}$ is the effective stripping, and 0.93 the active volume for $\alpha$. $N$ is the number of incident muons in each case (normalization to the high-energy coincident background was shown to be equivalent). We assume for now that both the number of $\mu^-$ stopped and the yield $\chi$ are proportional to $\phi$. (See the next section.) The result is $\omega_s^o = (0.80 \pm 0.14)\%$ (statistical error).

$\omega_s^o$ measured in the 650-Torr experiment is $(0.91 \pm 0.3)\%$ (statistical error).[19] The error is larger since fewer $(\alpha\mu)^+$ were observed in the presence of substantial background.

## SYSTEMATIC UNCERTAINTY

We now examine systematic uncertainties for items in Table II listed under "*Separate $D-T$ fills for $(\alpha\mu)^+$ and $\alpha$*". The $t\mu$ and $d\mu$ diffusion distances are limited by the muon lifetime at such low pressures and could become somewhat longer due to diffusion while the atoms are still epithermal. We estimate this distance to be about 1 cm at 490 Torr, somewhat smaller than the dimensions of the target. No correction is made at this time; generalization of Cohen's solution to the time-dependent Boltzmann equation[20] to get the spatial extent would be appropriate for a good estimate.

The most important uncertainty is a consequence of the use of two different densities in making the measurements. At our densities thermalization times equal or exceed the muon lifetime. Therefore most of the molecular formation will occur in the epithermal (transient) region where $\lambda_{dt\mu}$ is rapidly changing, and the yield $\chi$ may then not scale with density as assumed above. Table V attempts to outline the scope of this problem. Thermalization times, as well as average temperature and remaining triplet fraction at a relevant time of 2 $\mu s$ (all from ref. 20) tell us that at the lowest density the $t\mu$ atoms remain hot, and the triplet quenching is not complete. The muon lifetime then selects rather different slices of the epithermal transient for each density. (See survey of experimental low-density transients in refs. 21 and 22 and calculated transient effects in ref. 23)

TABLE V. Density Effect.

| *QUANTITY* | 490 *Torr* | 1800 *Torr* |
|---|---|---|
| *Density* $\phi$ | $7.6 \times 10^{-4}$ | $2.8 \times 10^{-3}$ |
| *Thermalization time* | 6 $\mu s$ | 1.6 $\mu s$ |
| *Average temperature at 2* $\mu s$ | $540K$ | $340K$ |
| $t\mu$ *triplet fraction at 2* $\mu s$ | 0.33 | 0.04 |
| *Average* $\lambda_{dt\mu}$ | $1.5 \times 10^8$ | $1.3 \times 10^8$ |
| *Extrapolated* $q_{1s}$ *from ref.*26 | 0.77 | 0.66 |

Next, let's see how large the effect is likely to be. Turning to Leon[24] to estimate singlet and triplet formation rates for our mixture at the two average temperatures, we find a higher rate for the less-thermalized, low-density case. The rates given in the Table V do not include screening effects,[25] but these will not alter the relative magnitudes. Nor should extension to the theory of direct molecular formation[23] seriously alter the relative magnitudes since the molecular-formation rates as a function of temperature still have similar shapes.

Other quantities remaining for discussion are $q_{1s}$ and $\lambda_{10}$. An extrapolation of the Menshikov and Ponomarev $q_{1s}$ is presented in Table V for each density[26];

here the strongest density dependence is predicted at low density. The direction of the $q_{1s}$ density dependence is to offset the increased formation rate expected at the low density. In this simplified treatment, the 0.33 triplet fraction remaining in the 490 Torr sample has little effect on the conclusion; in the event that $\lambda_{10}$ is actually larger than calculated[27], the triplet fraction could approach zero without largely affecting the $\lambda_{dt\mu}$ listed in the table.

Some comments are in order: 1) Expected epithermal enhancement of $\lambda_{dt\mu}$ makes the $q_{1s}$ density dependence more important in determining yield at $C_t = 0.4$. Hence the RAL experiment may find a larger optimum $C_t$ where the higher yield would be welcome. 2) $\lambda_{10}$ effects would likely enter in a important way if a proper evaluation over the complete epithermal peak were done. 3) Thermalization could be more rapid than reported. 4) We should pay attention to the plunging cycle rates at low density,[4,5] keeping in mind that the lowest-density points ($\phi$=1%) are already heavily into the epithermal region. But simply taking $\chi = \phi\lambda_c/\lambda_o = 0.08/\mu^-$ (450 Torr) with $\lambda_c$ at $45/\mu$s gives a predicted rate for *our* experiment that agrees with the absolute number of muon stops in the mixture found by foil activation. Unfortunately the foil test disagrees badly (by a factor of 2) with the number of stops estimated from beam properties. We might otherwise have hoped to bracket the extent of the epithermal enhancement at low densities (subject to assumptions about gas purity). 5) We anticipate that the RAL pulsed-beam data will add to the understanding of this low density region and answer some of the questions raised by the LAMPF experiment.

The initial $C_t$ of 0.4 falls with time, and ionization chamber measurements indicate $C_t$ dropped to 0.38 at the end of the data collection on the first 1800 Torr fill and to 0.37 at the end of the 490-Torr data collection. This small change is significant only if the optimum $C_t$ is much higher so that 0.4 is on the rising edge of the $\lambda_c$ vs $C_t$ curve instead of at the plateau where we intended it to be.

Variations in $\omega_s^o$ depending on cuts used have been evaluated in the thesis of Li[19]; the rms scatter amounts to about 0.06% which we add to the statistical error. Based on the reliability of the above assumptions, we believe it unlikely that the density effect will alter $\omega_s^o$ by more than 15%. Accordingly a systematic uncertainty is quoted with the result: $\omega_s^o = (0.80 \pm 0.15 \pm 0.12$ systematic)% Subsequent experiments or calculations on the density effect can be used to correct this result.

The 650-Torr sticking measurement, as outlined in Table II, does not contain uncertainly due to the density effect, and its consistent value of $(0.91 \pm 0.3)$% (statistical error), adds confidence to our conclusion.

## CONCLUSION

In conclusion, we report a measurement of the initial $\alpha - \mu$ sticking probability in muon catalyzed $d - t$ fusion at low density. $\omega_s^o$, measured directly for the first time, is $(0.80 \pm 0.15 \pm 0.12$ systematic)% in agreement with 'standard'

theoretical calculations[28,29,30] and not supporting those theories that invoke special mechanisms to alter the initial sticking.[31,32,33] The reported value contains only a 16% correction to the observed sticking due to stripping. Additional experiments are underway at the Rutherford-Appleton Laboratory where a high-Z target in the pulsed muon beam produces lower backgrounds. Direct normalization to neutron singles, transient observation, and reactivation tests should be possible.

## ACKNOWLEDGEMENTS

We wish to thank R. H. Sherman of the Los Alamos National Laboratory for making a test of the cleanliness in tritium of the thin mylar coated with aluminum. Little impurity was seen in his Raman spectrometer, giving us confidence to proceed.

This work is supported by the U. S. Department of Energy Division of Advanced Energy Projects.

## REFERENCES

1. Panel discussion on the Future of $\mu$CF, C. Petitjean Chairman, Muon Cat. Fusion 1, 391 (1987)
2. S.E. Jones *et al.*, Phys. Rev. Lett. 56, 588, (1986).
3. C. Petitjean *et al.*, Muon Cat. Fusion 1, 89 (1987).
4. C. Petitjean *et al.*, Muon Cat. Fusion 2 37 (1988).
5. See both W. H. Breunlich and C. Petitjean, $\mu$CF Workshop, Sanibel Island (1988).
6. H. Bossy *et al.*, Phys. Rev. Lett. 59, 2864, (1987).
7. K. Nagamine *et al.*, Muon Cat. Fusion 1, 137 (1987).
8. J.S. Cohen, Phys. Rev. Lett. 58, 1407 (1987).
9. V. E. Markushin, Muon Cat. Fusion 3, 395 (1988).
10. A. A. Vorobyov, Muon Cat. Fusion 2 17 (1988).
11. G. Semenchuk, private communication (1986).
12. S. E. Jones *et al.*, Muon Cat. Fusion 1, 121 (1987).
13. J. Davies, $\mu$CF Workshop, Sanibel Island (1988).
14. N. C. Mukhopadhyay, Phys. Reports 30, 98, (1977).
15. A. J. Caffrey *et al.*, Muon Cat. Fusion 1, 53 (1987).
16. G. Heusser and T. Kirsten, Nucl Phys. *A*195, 369 (1972).
17. H. Bichsel, Private communication.
18. J.S. Cohen, Phys. Rev. *A*37, 2343 (1988).
19. P. Li, Thesis, Brigham Young University, unpublished (1988).
20. J.S. Cohen, Phys. Rev. *A*34, 2719 (1986).
21. W. H. Breunlich *et al.*, Muon Cat. Fusion 1, 67 (1987).
22. C. Petitjean *et al.*, Muon Cat. Fusion 2 37 (1988).
23. J. S. Cohen and M. Leon, Phys. Rev. Lett. 55, 52 (1985).

24. M. Leon, Phys. Rev. Lett. 52, 605(1984) and corrected figures in 52, 1655 (1984) (Caution is advised due to the emergence of the sub-threshold resonances as strong contributors to the molecular formation).
25. J. S. Cohen and R. L. Martin, Phys. Rev. Lett. 53, 738 (1984).
26. L. I. Menshikov and L. I. Ponomarev, Pisma Zh. Eksp. Teor. Fiz. 39, 542 (1984) [Sov. Phys. JETP Lett. 39, 663 (1984)].
27. M. Leon, $\mu$CF Workshop, Sanibel Island (1988).
28. L. N. Bogdanova *et al.*, Nucl Phys. *A*454, 653 (1986).
29. D. Ceperley and B. J. Alder, Phys. Rev. *A*31, 1999 (1985).
30. Chi-Yu Hu, Phys. Rev. *A*34, 2536 (1986).
31. J. Rafelski and B. Müller, Phys. Lett. 164*B*, 223 (1985).
32. M. Danos, B. Müller, and J. Rafelski, Muon Cat. Fusion 3 (1988).
33. M. Danos, L.C. Biedenharn, A. Stahlhofen, , $\mu$CF Workshop, Sanibel Island (1988).